RESEARCH ARTICLE

Impact of White Adipose Tissue on Brain Structure, Perfusion, and Cognitive Function in Patients With Severe Obesity

The BARICO Study

Debby Vreeken, MSc,* Florine Seidel, MSc,* Guido de La Roij, MSc, Wouter Vening, MD, Willem A. den Hengst, MD, PhD, Lars Verschuren, PhD, Serdar Özsezen, Msc, Roy P.C. Kessels, PhD, Marco Duering, MD, PhD, Henk J.M.M. Mutsaerts, MD, PhD, Robert Kleemann, PhD, Maximilian Wiesmann, PhD, Eric J. Hazebroek, MD, PhD,† and Amanda J. Kiliaan, PhD†

Correspondence
Dr. Kiliaan
amanda.kiliaan@radboudumc.nl

Neurology® 2023;100:e703-e718. doi:10.1212/WNL.0000000000201538

Abstract

Background and Objective

While underlying pathophysiology linking obesity to brain health is not completely understood, white adipose tissue (WAT) is considered a key player. In obesity, WAT becomes dysregulated, showing hyperplasia, hypertrophy, and eventually inflammation. This disbalance leads to dysregulated secretion of adipokines influencing both (cardio)vascular and brain health. Within this study, we investigated the association between omental WAT (oWAT) and subcutaneous WAT (scWAT) with brain structure and perfusion and cognition in adults with severe obesity.

Methods

Within the cross-sectional BARICO study, brain structure and perfusion and cognitive function were measured before bariatric surgery (BS) using MRI and cognitive assessments. During BS, oWAT and scWAT depots were collected and analyzed by histopathology. The number and diameter of adipocytes were quantified together with the amount of crown-like structures (CLS) as an indication of inflammation. Blood samples were collected to analyze adipokines and inflammatory markers. Neuroimaging outcomes included brain volumes, cortical thickness, white matter (WM) integrity, WM hyperintensities, cerebral blood flow using arterial spin labeling (ASL), and the ASL spatial coefficient of variation (sCoV), reflecting cerebrovascular health.

Results

Seventy-one patients were included (mean age 45.1 ± 5.8 years; 83.1% women; mean body mass index 40.8 ± 3.8 kg/m^2). scWAT showed more CLS ($z = -2.72$, $p < 0.01$, $r = -0.24$) and hypertrophy compared with oWAT ($F(1,64) = 3.99$, $p < 0.05$, $\eta^2 = 0.06$). Adiponectin levels were inversely associated with the average diameter of scWAT (β = −0.31, 95% CI −0.54 to −0.08) and oWAT (β = −0.33, 95% CI −0.55 to −0.09). Furthermore, the adipocyte diameter in oWAT was positively associated with the sCoV in the parietal cortex (β = 0.33, 95% CI 0.10–0.60), and the number of adipocytes (per mm^2) was positively associated with sCoV in the nucleus accumbens (NAcc) (β = 0.34, 95% CI 0.09–0.61). Cognitive function did not correlate with any WAT parameter or plasma marker. These associations were highly influenced by age and sex. sCoV in the NAcc was positively associated with fasting plasma glucose (β = 0.35, 95% CI 0.10–0.56).

*The authors contributed equally to this work as first authors.

†These authors contributed equally to this work as senior authors.

From the Department of Medical Imaging (D.V., F.S., G.L.R., M.W., A.J.K.), Anatomy, Radboud University Medical Center, Nijmegen, The Netherlands; Department of Bariatric Surgery (D.V., W.V., W.A.H., E.J.H.), Vitalys, Part of Rijnstate Hospital, Arnhem, The Netherlands; Donders Institute for Brain (D.V., F.S., R.P.C.K., M.W., A.J.K.), Cognition, and Behavior and Radboudumc Alzheimer Center, Radboud University Medical Center, Nijmegen, The Netherlands; Department of Metabolic Health Research (F.S., R.K.), Netherlands Organisation for Applied Scientific Research (TNO), Leiden; Department of Microbiology and Systems Biology (L.V., S.Ö.), Netherlands Organisation for Applied Scientific Research (TNO), Zeist; Vincent van Gogh Institute for Psychiatry (R.P.C.K.), Venray, The Netherlands; Department of Medical Psychology and Radboudumc Alzheimer Center (R.P.C.K.), Radboud University Medical Center, Nijmegen, The Netherlands; Medical Image Analysis Center (MIAC) and Qbig (M.D.), and Department of Biomedical Engineering, University of Basel, Switzerland; Department of Radiology and Nuclear Medicine (H.J.M.M.M.), Amsterdam UMC, Amsterdam Neuroscience, The Netherlands; and Division of Human Nutrition and Health (E.J.H.), Wageningen University, The Netherlands.

Go to Neurology.org/N for full disclosures. Funding information and disclosures deemed relevant by the authors, if any, are provided at the end of the article.

Glossary

ASL = arterial spin labeling; **ATT** = arterial transit time; **BMI** = body mass index; **BS** = bariatric surgery; **CBF** = cerebral blood flow; **COWAT** = Controlled Word Association Test; **CLS** = crown-like structure; **CRP** = C-reactive protein; **DWI** = diffusion-weighted imaging; **ELISAs** = enzyme-linked immunosorbent assays; **FPG** = fasting plasma glucose; **FLAIR** = fluid-attenuated inversion recovery; **GM** = gray matter; **HbA1c** = hemoglobin A1c; **ICV** = intracranial volume; **IQR** = interquartile range; **IL-6** = interleukin-6; **MoCA** = Montreal Cognitive Assessment; **MSMD** = mean skeletonized mean diffusivity; **nAcc** = nucleus accumbens; **ns** = not significant; **oWAT** = omental WAT; **ROI** = region of interest; **sCoV** = spatial coefficient of variation; **scWAT** = Subcutaneous WAT; **SAA** = serum amyloid A; **SIMOA** = single-molecule array; **TE** = echo time; **TI** = inversion time; **TR** = repetition time; **TAP** = Test of Attentional Performance; **TNF-α** = tumor necrosis factor alpha; **vWAT** = visceral WAT; **WAT** = white adipose tissue; **WC** = waist circumference; **WM** = white matter; **WMH** = white matter hyperintensity.

Discussion

scWAT and oWAT are different in morphology and in their relationship with plasma markers and cerebrovascular health. Although scWAT showed more CLS and hypertrophy, scWAT was not associated with brain readouts. This study showed, however, important relationships between oWAT morphology and cerebrovascular health in obesity.

Trial Registration Information

Trial Registration Number NTR7288 (trialregister.nl/trial/7090).

The incidence of obesity is increasing to pandemic levels forming a major health challenge.[1] Mid-life obesity affects brain structure and function leading to a higher risk of developing dementia (especially Alzheimer disease).[2]

Neuroimaging studies have shown that particularly cerebrovascular mechanisms link obesity and brain health. Cerebrovascular measures include cerebral blood flow (CBF) derived from arterial spin labeling (ASL) and corresponding arterial transit time (ATT) because a longer ATT may indicate a delay in oxygen and nutrient delivery.[3] The spatial coefficient of variation (sCoV) derived from CBF images can be used as a proxy of ATT and demonstrated to increase with cognitive decline.[3] Previous research described the relationship between obesity and lower cerebral autoregulatory capacity, which can lead to impaired CBF and subsequently to reduced brain volume and cognitive function.[4] Obesity is also independently associated with cortical thinning and brain volume changes including caudate nucleus, putamen, and nucleus accumbens (NAcc).[5-8] Last, obesity is linked to decreased white matter (WM) integrity and increased WM hyperintensity (WMH) burden, hallmarks for multiple vascular risk factors.[9,10] Altogether, these changes may lead to cognitive impairment.[11] The exact mechanisms how obesity may affect brain health are not well established, but proposed mechanisms include the role of white adipose tissue (WAT) and cerebrovascular health.[11]

WAT is not only involved in energy storage but also an endocrine organ regulating the secretion of adipokines and cytokines.[12] In obesity, WAT expansion is characterized by hypertrophy (enlarged adipocytes) and hyperplasia (increased number of adipocytes). These alterations in WAT morphology lead to an elevated recruitment of macrophages forming the so-called crown-like structures (CLS) surrounding dysfunctional or dying adipocytes. CLS are important hallmarks for WAT dysfunction contributing to a low-grade inflammation state.[13] In addition, these obesity-induced changes in WAT morphology result in a higher secretion of proinflammatory adipokines.[2,14] Adipokine secretion is fat depot specific and relates to differences in adipocyte morphology and inflammation. Subcutaneous WAT (scWAT), located underneath the skin, is assumed to secrete fewer and less proinflammatory cytokines compared with visceral WAT (vWAT).[13] vWAT surrounds the organs and can be divided into several depots, including more superficially located omental WAT (oWAT) and mesenteric WAT surrounding the intestines.[13] Overall, research indicates a predominant contribution of vWAT to systemic inflammation and obesity-associated metabolic diseases compared with scWAT.[15] Yet, fat depot–specific effects on brain structure and function in obesity remain unresolved.

Adipokines linked to obesity-related comorbidities are leptin, adiponectin, serum amyloid A (SAA), interleukin (IL)-6, and tumor necrosis factor alpha (TNF-α). The imbalance in obesity includes, e.g., high levels of leptin, IL-6, and TNF-α and low adiponectin levels.[16] These adipokines can affect brain structures by directly crossing the blood-brain barrier or through indirect pathways.[2] For example, SAA has adverse effects on the cardiovascular system by stimulating atherosclerosis,[17] contributing to changes in the circulation and consequently CBF. Altogether, this illustrates that WAT and secreted adipokines exert direct and indirect effects on the brain through vascular and systemic inflammation.

In this cross-sectional study, we examined the relationship between abdominal scWAT and oWAT morphology and

inflammation and brain MRI outcomes and cognitive function in adults with severe obesity enrolled in the BARICO study (BAriatric surgery Rijnstate and Radboudumc neuro-Imaging and Cognition in Obesity). We first analyzed possible differences in oWAT and scWAT histology and associations with inflammatory cytokines, adipokines, fasting plasma glucose (FPG), and hemoglobin A1c (HbA1c). The obtained datasets were then associated with brain structure and function (including cerebrovascular health, WM health, brain volume, cortical thickness, and cognition). To date, multiple studies explored the link between obesity and brain health or studied WAT depot–specific differences and effects on secreting adipokines in obesity.[5,6,9,10,13,14,18-22] However, the direct relationship between WAT morphology and brain function and structure is still unexplored. Identifying and understanding associations between WAT and brain health in obesity could reveal important underlying mechanisms.

Methods

Description of Study Population

The BARICO study investigates the effect of weight loss on brain structure and function after bariatric surgery (BS).[23] Patients aged between 35 and 55 years were recruited when eligible for Roux-en-Y gastric bypass. Exclusion criteria were as follows: neurologic or severe psychiatric illness earlier or during recruitment; pregnancy; and treatment with any antibiotics, probiotics, or prebiotics 3 months before or during the study (excluding preoperative prophylaxis). Extra exclusion criteria for MRI were as follows: claustrophobia; epilepsy; pacemakers and defibrillators; nerve stimulators; intracranial clips; infraorbital or intraocular metallic fragments; cochlear implants; ferromagnetic implants; circumference above MRI space capacity; color blindness; and left handedness (to create a more homogenous sample with less variance).

Four weeks before surgery, participants were assessed through medical evaluation, cognitive tests, and blood collection. During surgery, biopsies of scWAT and oWAT were collected. For this study, only individuals who underwent an MRI scan were included.

Standard Protocol Approvals, Registrations, and Patient Consents

The study was approved by the Medical Ethics Committee CMO region Arnhem–Nijmegen (NL63493.091.17) and by the local institutional ethics committee. The study was conducted in accordance with the Declaration of Helsinki "Ethical Principles for Medical Research Involving Human Subjects" and in accordance with the guidelines for Good Clinical Practice (CPMP/ICH/135/95). All participants provided written informed consent. The study was prospectively registered in the Netherlands Trial Registry (www.trialregister.nl: NTR7288).

Medical Examination

Anthropometric measurements included body weight, body mass index (BMI), waist circumference (WC), and blood pressure. BMI was calculated as weight divided by height in meters squared. Systolic and diastolic blood pressure was measured in sitting position. Hypertension was defined as the use of antihypertensive drugs and/or a blood pressure ≥130/80 mm Hg. Diabetes type 2 mellitus was defined by the use of oral antidiabetic or insulin medication and/or FPG of ≥7.0 mmol/L and HbA1c ≥ 48 mmol/mol, and prediabetes was defined by FPG ≥ 5.5 and <7.0 mmol/L and HbA1c ≥ 39 or <48 mmol/mol. Currently smoking was defined as smoking ≥1 cigarette per day.

Fasting blood samples were collected 4 weeks before surgery and on the day of surgery and stored at −80°C. Total leptin (pg/mL), adiponectin (μg/mL), C-reactive protein (CRP) (μg/mL), SAA (μg/mL), TNF-α (pg/mL), interleukin-1β (IL-1β) (pg/mL), and IL-6 (pg/mL) were determined with human enzyme-linked immunosorbent assays or single-molecule array technology using SP-X imaging system (Quanterix, Billerica, MA). To account for fluctuations in adipokines and inflammatory markers, average values of 2 measurements before and at surgery were used in the analyses.

WAT Histopathology

Abdominal scWAT and oWAT samples were collected during BS and immediately fixed in 4% formaldehyde for 24–48 hours. Samples were dehydrated overnight (Automatic Tissue Processor ASP300S, Leica Biosystems, Amsterdam, the Netherlands) and embedded in paraffin. 5-μm thick cross-sections were histologically stained with hematoxylin-eosin. All stained sections were digitized with an Aperio Digital Pathology Slide Scanner AT2 (Leica) at ×20 magnification. On the slide scans, 2–7 areas (250,000 μm^2 per area) containing intact WAT were randomly selected across the tissue and exported to TIFF with Aperio ImageScope slide viewer (Leica Biosystems). Using ImageJ (version 1.53, NIH) and established Adiposoft software (version 1.16),[24] adipocytes were automatically detected (excluding adipocytes on the edges) and adipocyte diameter (μm) was determined. The number of adipocytes per mm^2 and average adipocyte diameter (μm) were calculated. To assess inflammation, the number of CLS was manually quantified in the stained cross-sections by 2 independent blinded assessors using an Axioskop FS Neurolucida Microscope (Zeiss Microscopy, Jena, Germany) and Stereo Investigator software (version 2020, MBF Bioscience). CLS, defined as circular structures formed by inflammatory cells surrounding adipocytes, were included when at least 3 opposite nuclei surrounded the adipocyte or when the inflammatory aggregates comprised at least 50% of the adipocyte circumference. The total number of CLS per 1,000 mm^2 was finally calculated.

MRI Acquisition

Participants were scanned on a 3T Skyra scanner (Siemens Healthineers, Erlangen, Germany) using a 32-channel head

coil. The acquisition protocol included a 3D T1-weighted magnetization-prepared rapid gradient-echo sequence (repetition time [TR]/inversion time [TI]/echo time [TE] 2300/1100/3.03 ms; 8° flip angle; and voxel size: 1 mm isotropic), a 3D fluid-attenuated inversion recovery (FLAIR) sequence (TR/TI/TE 5000/1800/397 ms; 120° flip angle; and voxel size: 1 mm isotropic), a pulsed arterial spin labeling (ASL) sequence (PICORE, bolus duration: 700 ms; TI: 1,800 ms) with 2D echo-planar imaging readout (TR/TE 2,500/12 ms; voxel size: 4 × 4mm, 9 slides of 8 mm with a 2-mm slice gap, 45 control-label pairs, no background suppression, mean control used as M0), and diffusion-weighted imaging (DWI) MRI scans using multiband echo-planar imaging (TR/TE 3275/91.4 ms; voxel size: 1.9 mm isotropic; 6× b = 0 s/mm^2, 42× b = 900 s/mm^2, 83× b = 1800 s/mm^2).

MRI Outcomes and Image Processing

Brain Volume and Cortical Thickness

Cortical reconstruction and volumetric segmentation were performed using default settings in the Freesurfer Imaging Analysis Suite (v.6.0.0),[25] described in detail elsewhere.[26] Global measures included the following: total cerebral gray matter (GM) and WM volume (based on the percentage of intracranial volume) and overall mean cortical thickness. Regional measures included subcortical volumetric measures (thalamus, caudate nucleus, putamen, NAcc, hippocampus, and amygdala) and cortical volumes and thickness measures of the following a priori selected region of interests (ROIs) from merged Desikan-Killiany atlas ROIs[27]: cingulate gyrus, insula, and frontal, occipital, parietal, and temporal cortex.

White Matter Hyperintensities and Integrity

WMHs of presumed vascular origin, as defined by consensus criteria,[28] were segmented using a fully automated, deep learning algorithm based on multidimensional gated recurrent units with 3D FLAIR and 3D T1-weighted images as input.[29] Output segmentation masks were quality controlled by visual inspection and used to determine WMH count and volume.

Multidirectional DWI data were processed with the Functional Magnetic Resonance Imaging of the Brain software library (FSL; v6.0.1).[30] Quality assessment was conducted using the FSL eddy tool Quality Assessment for DWI (eddy_quad) and through visual inspection of all images. DWI data were denoised using Marchenko-Pastur principal component analysis, and Gibbs artifacts were removed (MRtrix3 package, version 3.0.0, dwidenoise,[31-33] and mrdegibbs[33,34]). Afterward, DWI images were corrected for susceptibility and eddy current–induced distortions and head motion using the topup and eddy_correct tools of FSL. The diffusion tensor imaging metrics were calculated using dtifit (FSL). The mean skeletonized MD (MSMD) parameter was computed fully automated using a shell script,[35] described in detail elsewhere.[36] The WMH mask was used to measure tensor metrics only in normal-appearing WM (i.e., outside of WMH).

Arterial Spin Labeling

Postprocessing of ASL images was performed with toolbox ExploreASL,[37] version 1.5.1., including SPM 12, version 7219 (Statistical Parametric Mapping, Wellcome Trust Centre for Neuroimaging, London, United Kingdom), CAT12 version r1615, and LST, version 2.0.15. This software was used with Matlab, version 2020a (MathWorks, MA). Complete processing steps are described in detail elsewhere.[37] Scans of insufficient quality due to excessive head motion were excluded. In total, 4 male participants (5.6%) with relatively large head size were excluded because the use of a necessary smaller cushion caused more head motions.

CBF (ml/100 g/min) and sCoV (%) within overall cerebral GM and several ROIs were calculated. sCoV was defined as the standard deviation divided by the mean CBF.[38] A priori, the following ROIs based on literature were prespecified combining the Harvard-Oxford[27] and MNI structural atlas[39]: thalamus, caudate nucleus, putamen, NAcc, cingulate gyrus, insula, and frontal, occipital, parietal, and temporal cortex. Unfortunately, due to field of view, we were not able to include more ventral located regions such as hippocampus and amygdala. CBF and sCoV were calculated both with and without partial volume correction for overall GM and each ROI.[37]

Cognitive Outcomes

Cognitive performance was assessed with multiple neuropsychological tests, described in detail elsewhere.[23] General cognitive performance was assessed by the Montreal Cognitive Assessment (MoCA).[40] The Digit Span test (Wechsler[41] Adult Intelligence Scale-Fourth Edition) was used to determine working memory. Episodic memory was assessed through the immediate and delayed Story Recall test from the Rivermead Behavioral Memory test.[42] The Controlled Oral Word Association Test was used to determine verbal fluency.[43] Last, the Flexibility subtest from the computerized Tests of Attentional Performance (2.3) was used to study ability to shift attention.[44] We used a compound score for global cognitive function as an outcome measure. This score was calculated by taking the mean of the *z* scores of the natural log transformation of the MoCA score, the flexibility subtest score from the Tests of Attentional Performance, the added score of 3 trials (forward, backward, and sorting) of the Digit Span test, the total score of the verbal fluency, and the added score of the immediate and delayed story recall test. The level of education was determined through the Verhage score based on the Dutch education system (1 = lowest, i.e., less than primary school, and 7 = highest level of education, i.e., a university degree).[45]

Statistical Analyses

Cross-sectional descriptive analyses between men and women were performed. To test differences between WAT depots, univariate analysis of variance was used and controlled for age and sex. When assumptions on normality and homogeneity

were not met, a natural log or reciprocal transformation or nonparametric tests were used.

The relationship between WAT parameters, plasma markers, and brain structure and perfusion were determined with linear regression models. Effects of confounding variables on the associations were explored using 4 models: no adjustments (crude model), adjustments for age (model 2), additional adjustments for sex (model 3), and a full model with adjustments for age, sex, education, HT, DM, and smoking (full model). As sensitivity analysis, we repeated the analyses in women only. Hematocrit and head motion during the ASL sequence were both considered as potential covariates for sCoV and CBF, and head motion was also considered as a potential covariate for MSMD. However, the variables were not associated with GM sCoV, GM CBF, or MSMD ($p > 0.05$); therefore, we did neither control for hematocrit nor head motion. The regression analyses were only performed for partial volume–corrected ASL data.

Statistical analyses were conducted in IBM SPSS statistics, version 25 (SPSS Inc., Chicago, IL). Alpha was set at 0.05 (2-tailed) for the descriptive analyses and differences between WAT depots. For the regression analyses, alpha was set at 0.01 (2-tailed).

Data Sharing Statement

De-identified data from the BARICO study will be made available on request after approval by the study investigators.

Results

Descriptive Statistics

In total, 71 individuals were included in our analysis (eFigure 1, links.lww.com/WNL/C471). Participant characteristics are listed in Table 1; the mean age of the participants was 45.1 ± 5.8 years with a mean BMI of 40.8 ± 3.8 kg/m^2 and a mean WC of 122.2 ± 10.4 cm. Approximately 83.1% of the study population were women.

Relationship Between WAT Morphology, Inflammation, and Circulating Plasma Makers

oWAT contained a higher number of adipocytes per mm^2 ($p = 0.017$; $F(1,64) = 6.03$), a lower average diameter of adipocytes ($p = 0.050$; $F(1,64) = 3.99$), and less CLS ($Z = -2.72$, $p = 0.007$) compared with scWAT (Figure 1).

Plasma adiponectin was positively associated with adipocyte number in scWAT and inversely associated with average adipocyte diameter in both depots in the crude model and after adjustment for age (Table 2). After additional adjustment for sex, the associations between average adipocyte diameter and adiponectin were nonsignificant. Higher plasma adiponectin was associated with an increased number of adipocytes in scWAT and a lower average adipocyte diameter in both depots in the crude model and after adjustment for age.

In a sensitivity analysis in women only, the association between WAT morphology and adiponectin attenuated, and higher CRP was associated with a decreased number of adipocytes and a larger average adipocyte diameter in oWAT (eTable 3A, links.lww.com/WNL/C471). Furthermore, higher SAA was associated with a larger adipocyte diameter in oWAT in the crude model only.

Relationship Between WAT Parameters and Brain Structure and Perfusion

We examined the association between WAT morphology, inflammation, and main neuroimaging and cognition parameters (Table 3). Figure 2 shows CBF and sCoV maps in 6 participants with the lowest and highest CBF. WAT parameters were not significantly associated with overall structural brain parameters or global cognitive function (Table 3).

However, the number and average diameter of adipocytes in oWAT were positively associated with sCoV in the following a priori ROIs (Table 4, eFigure 2, links.lww.com/WNL/C471): parietal cortex and NAcc. In the crude model, a higher sCoV in the parietal cortex was associated with a larger average diamter in oWAT. After adjustments, these associations attenuated and became nonsignificant. Regarding the NAcc, an increased number of adipocytes in oWAT was associated with a higher sCoV after age adjustment. In the full model, this association was borderline significant ($p = 0.010$). Restricting the analysis to women strengthened the significant associations between the NAcc and oWAT morphology (eTable 4).

Other a priori ROIs for brain volume and cortical thickness or cognitive function did not correlate significantly with WAT parameters (data not shown). Subsequently, we explored whether the relationship between WAT-associated brain parameters is driven by plasma markers (eTable 5, links.lww.com/WNL/C471). Higher FPG levels were associated with a higher sCoV in the NAcc, in the crude model (no adjustments), adjusted for age (model 2), and additionally adjusted for sex (model 3). No other significant associations between sCoV in parietal cortex and NAcc and plasma markers were discovered.

Last, we explored the relationship between cognitive parameters and plasma markers. No significant associations were observed (eTable 6, links.lww.com/WNL/C471).

Discussion

This study examined the associations between scWAT and oWAT morphology, circulating plasma markers and brain structure and perfusion and cognition of persons with severe obesity included in the BARICO study. We observed more CLS and hypertrophy and less hyperplasia in scWAT compared with oWAT. Despite more CLS and hypertrophy, no associations between scWAT parameters and brain structure and cognition were observed. The average adipocyte diameter in oWAT was positively associated with sCoV in the parietal

Table 1 Characteristics of Participants

	All participants (n = 71[a])	Women (n = 59[a])	Men (n = 12[a])	*p* Value
Age, mean ± SD, y	45.1 ± 5.8	44.5 ± 5.8	48.0 ± 5.0	ns
Sex, women, n (%)	59 (83.1%)			
Height, mean ± SD, m	1.70 ± 0.07	1.68 ± 0.05	1.81 ± 0.04	<0.001
Weight, mean ± SD, kg	118.3 ± 14.5	115.1 ± 11.7	134.2 ± 16.9	<0.001
BMI, mean ± SD, kg/m^2	40.8 ± 3.8	40.8 ± 3.8	40.7 ± 3.8	ns
WC, mean ± SD, cm	122.2 ± 10.4	119.9 ± 9.0	134.1 ± 9.4	<0.001
Level of education[b], n (%)				
Low	9 (12.7)	6 (10.2%)	3 (25.0%)	ns
Middle	36 (50.7%)	30 (50.8%)	6 (50.0%)	ns
High	26 (36.6%)	23 (39.0%)	3 (25.0%)	ns
Comorbidities, n (%)				
Diabetes mellitus	12 (16.9%)	9 (15.3%)	3 (25.0%)	ns
Prediabetes	6 (8.5%)	5 (8.5%)	1 (8.3%)	ns
Hypertension	46 (64.8%)	34 (57.6%)	12 (100%)	<0.01
Smoking current, n (%)	10 (14.1%)	10 (16.9%)	0 (0.0%)	ns
Consuming alcohol, n (%)	20 (28.2%)	14 (23.7%)	6 (50.0%)	ns
Alcohol consumption, median (IQR), units per week	1 (1)	1 (1)	1 (2)	ns
Blood pressure, mean ± SD				
Systolic (mm HG)	135.3 ± 16.3	134.1 ± 16.4	140.9 ± 15.4	ns[c]
Diastolic (mm HG)	84.6 ± 8.8	84.1 ± 8.6	87.3 ± 9.7	ns[c]
HbA1c, median (IQR), mmol/mol	37.0 (7.0)	36.0 (6.0)	39.0 (11.5)	ns
FPG, median (IQR), mmol/L	5.7 (1.6)	5.6 (1.0)	6.7 (1.5)	ns
GM sCoV, mean ± SD, %	45.8 ± 14.7	45.3 ± 14.7	49.5 ± 15.3	ns
GM CBF, mean ± SD, ml/100g/minute	31.9 ± 5.8	31.9 ± 6.0	32.2 ± 4.0	ns
WMH, median (IQR)				
Volume (mL)	0.14 (0.31)	0.13 (0.30)	0.14 (0.43)	ns
Count	6 (5)	5 (6)	6 (2)	ns
MSMD, mean ± SD, 10^{-4} mm^2/second	3.34 ± 0.11	3.34 ± 0.11	3.36 ± 0.07	ns
Brain volume, mean				
GM (%ICV)	40.3 ± 3.4	40.6 ± 3.5	38.2 ± 1.2	<0.05
Hippocampus (%ICV)	0.55 ± 0.05	0.55 ± 0.05	0.54 ± 0.03	ns
Overall mean cortical thickness, mean ± SD, mm	2.45 ± 0.08	2.46 ± 0.08	2.42 ± 0.08	ns
Cognition, mean ± SD				
MoCA score, median (IQR)	27 (3)	27 (3)	26 (3)	ns
Digit Span (sum of Forward, Backward and Sorting)	26.6 ± 5.1	26.9 ± 5.3	25.2 ± 4.2	ns
Story Recall (sum of immediate and delayed recall)	16.7 ± 7.0	17.0 ± 7.4	15.1 ± 5.2	ns

Continued

Table 1 Characteristics of Participants *(continued)*

	All participants (n = 71[a])	Women (n = 59[a])	Men (n = 12[a])	*p* Value
COWAT	37.8 ± 10.4	38.5 ± 10.9	34.0 ± 7.0	ns
TAP Flexibility index score	−0.76 ± 6.8	−0.43 ± 6.5	−2.38 ± 8.1	ns

Abbreviations: BMI = body mass index; CBF = cerebral blood flow; COWAT = Controlled Word Association Test; FPG = fasting plasma glucose; GM = gray matter; HbA1c = hemoglobin A1c; ICV = intracranial volume; IQR = interquartile range; MoCA = Montreal Cognitive Assessment; MSMD = mean skeletonized mean diffusivity; ns = not significant; sCoV = spatial coefficient of variation; TAP = Test of Attentional Performance.; WC = waist circumference; WM = white matter; WMH = white matter hyperintensity.
Missing data: WC, n = 10 (14.1%).
p value of difference between men and women based on the independent sample *t* test, the Mann-Whitney *U* test, or the chi-square test.
eTable 2, links.lww.com/WNL/C471, summarizes all the imaging characteristics per region of interest.
[a] More information on the exact number of participants for each imaging parameter and cognitive test is shown in eFigure 1, links.lww.com/WNL/C471.
[b] Verhage score ≤4 is defined a low level of education, a Verhage score of 5 as middle, and a Verhage score of 6 or 7 as high.[45].
[c] Controlled for use of antihypertensive drugs.

cortex. The number of adipocytes analyzed per mm^2 in oWAT was positively associated with sCoV in the NAcc. These associations were highly influenced by age and sex. Figure 3 shows a schematic summary of the main results.

Multiple other human studies on obesity show a larger average adipocyte diameter in scWAT compared with oWAT.[18,19] The preferential site of fat storage is the scWAT depot. When the storage capacity of scWAT reaches a limit or when this depot is unable to store lipids because of insulin insensitivity, the condition may lead to accumulation of fat in the oWAT.[18] This, and the differential expression of perilipin between depots, might explain why scWAT showed an increased adipocyte diameter[46] (and references therein).

Endorsing our results, hypertrophic cells were associated with a more proinflammatory profile.[14] However, another study on severe obesity found higher macrophage infiltration in oWAT compared with scWAT.[20] These contradictory findings might be explained by 2 factors. First, differences in study populations regarding age, sex, and BMI might explain some of the variations between results. For example, the differences

Figure 1 Photomicrographs of Hematoxylin-Eosin–Stained Adipocyte Morphology and Morphology Differences Between Subcutaneous and Omental WAT

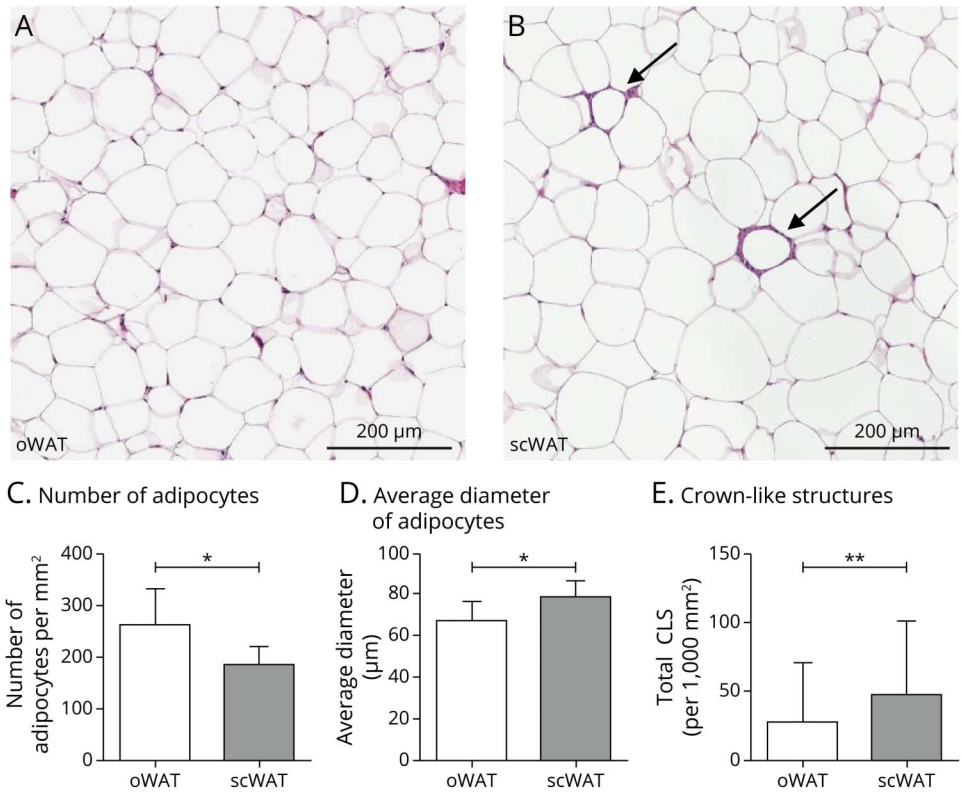

(A–B) Representative pictures of adipocytes in oWAT (A) and subcutaneous WAT (B) including crown-like structures (CLS) (indicated with arrows). (C) Number of adipocytes per mm^2 in omental and subcutaneous WAT. (D) Average diameter of adipocytes (µm) in omental and subcutaneous WAT. (E) Total number of CLS per 1,000 mm^2 in omental and subcutaneous WAT. Data are presented in mean ± SD. *$p < 0.05$, **$p < 0.01$. Analyses between oWAT and scWAT based on the number of adipocytes, diameter of adipocytes was controlled for age and sex. More information on the exact number of participants for each WAT parameter is summarized in eTable 2, links.lww.com/WNL/C471. Abbreviations: oWAT = omental white adipose tissue; scWAT = subcutaneous white adipose tissue.

Table 2 Linear Regression Models Estimating the Relationship Between Omental and Subcutaneous WAT and Plasma Markers

	Omental WAT			Subcutaneous WAT		
	Number of adipocytes per mm^2	Average diameter (μm)	CLS	Number of adipocytes per mm^2	Average diameter (μm)	CLS
	β (95% CI)	β (95% CI)	β (95% CI)	β (95% CI)	β (95% CI)	β (95% CI)
Leptin (pg/mL)						
Crude model	0.20 (−0.04 to 0.43)	−0.29 (−0.45 to 0.01)	−0.10 (−0.33 to 0.13)	0.12 (−0.12 to 0.36)	−0.12 (−0.36 to 0.13)	−0.11 (−0.37 to 0.14)
Adjusted for age	0.17 (−0.07 to 0.40)	−0.20 (−0.43 to 0.05)	−0.08 (−0.31 to 0.15)	0.11 (−0.13 to 0.36)	−0.11 (−0.35 to 0.14)	−0.10 (−0.36 to 0.15)
Adjusted for age and sex	−0.04 (−0.25 to 0.17)	0.05 (−0.17 to 0.26)	0.03 (−0.16 to 0.22)	−0.03 (−0.24 to 0.18)	0.02 (−0.19 to 0.22)	−0.07 (−0.28 to 0.14)
Full model	0.00 (−0.21 to 0.22)	0.01 (−0.20 to 0.23)	−0.06 (−0.25 to 0.14)	−0.05 (−0.25 to 0.15)	0.04 (−0.16 to 0.24)	−0.08 (−0.29 to 0.12)
Adiponectin (μg/mL)						
Crude model	0.27 (0.03–0.50)	−0.33[a] (−0.55 to −0.09)	−0.19 (−0.43 to 0.05)	0.34[a] (0.11–0.57)	−0.31[a] (−0.54 to −0.08)	−0.15 (−0.40 to 0.10)
Adjusted for age	0.28 (0.04–0.52)	−0.35[a] (−0.58 to −0.10)	−0.19 (−0.43 to 0.06)	0.34[a] (0.11–0.57)	−0.31 (−0.54 to −0.07)	−0.14 (−0.40 to 0.11)
Adjusted for age and sex	0.16 (−0.09 to 0.40)	−0.22 (−0.46 to 0.04)	−0.11 (−0.34 to 0.12)	0.26 (0.04–0.49)	−0.28 (−0.47 to −0.01)	−0.12 (−0.36 to 0.12)
Full model	0.18 (−0.08 to 0.42)	−0.24 (−0.49 to 0.01)	−0.17 (−0.41 to 0.07)	0.25 (0.02–0.47)	−0.24 (−0.47 to −0.02)	−0.18 (−0.42 to 0.04)
CRP (μg/mL)						
Crude model	−0.25 (−0.49 to −0.02)	0.27 (0.03–0.50)	0.00 (−0.25 to 0.25)	0.02 (−0.22 to 027)	−0.02 (−0.27 to 0.22)	−0.03 (−0.29 to 0.22)
Adjusted for age	−0.26 (−0.51 to −0.01)	0.28 (0.03–0.52)	−0.01 (−0.26 to 0.24)	0.03 (−0.21 to 0.28)	−0.03 (−0.28 to 0.21)	−0.04 (−0.30 to 0.22)
Adjusted for age and sex	−0.39[a] (−0.64 to −0.13)	0.43[a] (0.18–0.69)	0.03 (−0.22 to 0.29)	−0.02 (−0.27 to 0.23)	0.01 (−0.24 to 0.26)	−0.02 (−0.28 to 0.23)
Full model	−0.31 (−0.56 to −0.07)	0.37[a] (0.13–0.61)	0.00 (−0.24 to 0.25)	−0.05 (−0.29 to 0.18)	0.06 (−0.17 to 0.29)	0.01 (−0.23 to 0.25)
SAA (μg/mL)						
Crude model	−0.13 (−0.37 to 0.11)	0.12 (−0.13 to 0.36)	−0.10 (−0.34 to 0.14)	−0.03 (−0.27 to 0.21)	0.02 (−0.23 to 0.26)	−0.04 (−0.29 to 0.21)
Adjusted for age	−0.08 (−0.33 to 0.17)	0.06 (−0.19 to 0.31)	−0.12 (−0.36 to 0.11)	0.00 (−0.24 to 0.24)	−0.02 (−0.25 to 0.22)	−0.06 (−0.30 to 0.19)
Adjusted for age and sex	−0.20 (−0.45 to 0.05)	0.21 (−0.05 to 0.46)	−0.08 (−0.31 to 0.16)	−0.07 (−0.31 to 0.16)	0.05 (−0.19 to 0.28)	−0.04 (−0.28 to 0.20)
Full model	−0.21 (−0.47 to 0.06)	0.22 (−0.05 to 0.48)	−0.09 (−0.33 to 0.17)	−0.07 (−0.30 to 0.17)	0.05 (−0.18 to 0.28)	0.01 (−0.23 to 0.25)
TNF-α (pg/mL)						
Crude model	−0.16 (−0.41 to 0.08)	0.17 (−0.08 to 0.42)	−0.01 (−0.25 to 0.24)	0.01 (−0.29 to 0.26)	−0.04 (−0.28 to 0.20)	0.07 (−0.17 to 0.32)
Adjusted for age	−0.13 (−0.38 to 0.13)	0.13 (−0.12 to 0.39)	−0.03 (−0.27 to 0.22)	0.04 (−0.20 to 0.28)	−0.07 (−0.31 to 0.18)	0.06 (−0.19 to 0.30)
Adjusted for age and sex	−0.17 (−0.45 to 0.10)	0.19 (−0.09 to 0.47)	−0.02 (−0.27 to 0.24)	0.02 (−0.23 to 0.27)	−0.05 (−0.30 to 0.20)	0.06 (−0.18 to 0.31)
Full model	−0.16 (−0.46 to 0.13)	0.18 (−0.12 to 0.47)	−0.01 (−0.29 to 0.26)	0.02 (−0.24 to 0.29)	−0.05 (−0.31 to 0.21)	0.07 (−0.19 to 0.33)
IL-1β (pg/mL)	−0.20	0.15	−0.03	0.05	−0.07	−0.05
Crude model	−0.20 (−0.40 to 0.04)	0.15 (−0.09 to 0.36)	−0.03 (−0.28 to 0.22)	0.05 (−0.19 to 0.30)	−0.07 (−0.31 to 0.18)	−0.05 (−0.31 to 0.20)
Adjusted for age	−0.22 (−0.43 to 0.03)	0.17 (−0.08 to 0.39)	−0.02 (−0.27 to 0.23)	0.04 (−0.20 to 0.29)	−0.05 (−0.30 to 0.19)	−0.05 (−0.30 to 0.21)
Adjusted for age and sex	−0.17 (−0.40 to 0.09)	0.11 (−0.16 to 0.35)	−0.06 (−0.31 to 0.20)	0.09 (−0.16 to 0.34)	−0.09 (−0.34 to 0.15)	−0.06 (−0.31 to 0.20)
Full model	−0.13 (−0.38 to 0.15)	0.07 (−0.20 to 0.33)	−0.07 (−0.35 to 0.20)	0.09 (−0.17 to 0.35)	−0.09 (−0.36 to 0.17)	−0.07 (−0.33 to 0.20)

Continued

Table 2 Linear Regression Models Estimating the Relationship Between Omental and Subcutaneous WAT and Plasma Markers *(continued)*

	Omental WAT			Subcutaneous WAT		
	Number of adipocytes per mm^2	Average diameter (μm)	CLS	Number of adipocytes per mm^2	Average diameter (μm)	CLS
	β (95% CI)	β (95% CI)	β (95% CI)	β (95% CI)	β (95% CI)	β (95% CI)
IL-6 (pg/mL)						
Crude model	−0.13 (−0.36 to 0.10)	0.17 (−0.07 to 0.39)	−0.05 (−0.28 to 0.19)	0.01 (−0.24 to 0.25)	−0.01 (−0.25 to 0.24)	−0.07 (−0.32 to 0.18)
Adjusted for age	−0.08 (−0.31 to 0.16)	0.11 (−0.13 to 0.35)	−0.08 (−0.30 to 0.16)	0.04 (−0.20 to 0.27)	−0.04 (−0.28 to 0.19)	−0.09 (−0.34 to 0.15)
Adjusted for age and sex	−0.10 (−0.35 to 0.16)	0.15 (−0.12 to 0.40)	−0.07 (−0.31 to 0.16)	0.03 (−0.21 to 0.27)	−0.03 (−0.28 to 0.21)	−0.09 (−0.34 to 0.15)
Full model	−0.03 (−0.28 to 0.22)	0.10 (−0.16 to 0.35)	−0.14 (−0.37 to 0.09)	−0.01 (−0.24 to 0.22)	0.03 (−0.20 to 0.26)	−0.09 (−0.32 to 0.15)
FPG (mmol/L)						
Crude model	−0.15 (−0.40 to 0.10)	0.17 (−0.08 to 0.42)	0.06 (−0.19 to 0.31)	−0.04 (−0.26 to 0.18)	0.03 (−0.19 to 0.25)	0.00 (−0.23 to 0.23)
Adjusted for age	−0.06 (−0.31 to 0.18)	0.08 (−0.17 to 0.32)	0.02 (−0.21 to 0.26)	−0.00 (−0.21 to 0.21)	−0.01 (−0.22 to 0.20)	−0.02 (−0.24 to 0.20)
Adjusted for age and sex	−0.05 (−0.31 to 0.22)	0.06 (−0.21 to 0.33)	0.01 (−0.23 to 0.25)	0.03 (−0.19 to 0.24)	−0.04 (−0.25 to 0.18)	−0.03 (−0.24 to 0.19)
Full model	−0.04 (−0.22 to 0.15)	0.07 (−0.12 to 0.26)	0.10 (−0.07 to 0.27)	0.12 (−0.03 to 0.26)	−0.14 (−0.27 to 0.02)	0.05 (−0.11 to 0.19)
HbA1c (mmol/mol)						
Crude model	−0.23 (−0.48 to 0.01)	0.23 (−0.01 to 0.47)	0.07 (−0.18 to 0.32)	−0.13 (−0.34 to 0.10)	0.13 (−0.10 to 0.33)	0.02 (−0.21 to 0.25)
Adjusted for age	−0.13 (−0.37 to 0.10)	0.12 (−0.12 to 0.36)	0.02 (−0.21 to 0.25)	−0.09 (−0.28 to 0.13)	0.07 (−0.14 to 0.27)	−0.01 (−0.22 to 0.21)
Adjusted for age and sex	−0.14 (−0.40 to 0.11)	0.13 (−0.13 to 0.39)	0.02 (−0.22 to 0.25)	−0.07 (−0.28 to 0.15)	0.06 (−0.15 to 0.27)	−0.01 (−0.22 to 0.20)
Full model	−0.13 (−0.28 to 0.01)	0.13 (−0.01 to 0.28)	0.11 (−0.02 to 0.25)	0.02 (−0.11 to 0.14)	−0.02 (−0.14 to 0.10)	0.08 (−0.05 to 0.20)

Abbreviations: CLS = crown-like structures; CRP = C-reactive protein; FPG = fasting plasma glucose; HbA1c = hemoglobin A1c; IL-1β = interleukin-1β; IL-6 = interleukin-6; SAA = serum amyloid A; TNF-α = tumor necrosis factor alpha; WAT = white adipose tissue.
Beta coefficients with 95% confidence intervals. In the full model, we adjusted for age, sex, education, HT, DM, and smoking.
[a] p value < 0.01.

might be due to obesity stage because in an early stage, more fat accumulates in scWAT, leading to more CLS in scWAT. Another study in mid-life adults without obesity also showed higher macrophage infiltration in scWAT compared with oWAT.[21] Second, the fact that CLS mainly consist of M1 macrophages might also explain some of the variations. A higher number of M1 macrophages in scWAT is reported in men who are obese compared with almost all other inflammatory cell populations (e.g., B cells, T cells, and M2 macrophages), which were higher in oWAT.[22] Therefore, for further research, it is advised to measure other types of inflammatory cells in WAT instead of only CLS.

Earlier research showed strong correlations between scWAT cell size and leptin, adiponectin, IL-1β, IL-6, and TNF-α in overweight adults.[14] Contrastingly, we found only an inverse association between adipocyte diameter and a positive association with adipocyte number in scWAT and adiponectin. In oWAT, a positive association between CRP and average adipocyte diameter was also observed. Unexpectedly, we did not find associations with other plasma markers, which might be due to the relatively small adipocyte diameter in our study sample.[18] Another difference is that the variation in BMI is within the high segment (35–53 kg/m^2), whereas studies reporting associations typically compare low BMI with individuals who are overweight and obese. We focused only on the relationship between oWAT and scWAT and circulating plasma levels, and therefore, for further research, it is advised to include adipokine and chemokine secretion from adipocytes additionally to circulating plasma levels.

Human studies investigating the relationship between brain health, morphology, and inflammation in different WAT depots are rare. To date, studies have mainly focused on the relationship between other obesity indices (mainly BMI) and brain structure and function.[5,6,9,10] In this study, cerebrovascular health in the parietal cortex and NAcc was associated with oWAT morphology. Possibly, the relationship of WAT

Table 3 Linear Regression Models Estimating the Relationships Between Omental and Subcutaneous WAT Parameters and Neuroimaging Parameters and Global Cognition

	Omental WAT			Subcutaneous WAT		
	Number of adipocytes per mm^2	Average diameter (μm)	CLS	Number of adipocytes per mm^2	Average diameter (μm)	CLS
	β (95% CI)	β (95% CI)	β (95% CI)	β (95% CI)	β (95% CI)	β (95% CI)
GM sCoV (%)						
Crude model	−0.13 (−0.39 to 0.13)	0.16 (−0.10 to 0.44)	0.05 (−0.20 to 0.31)	0.09 (−0.16 to 0.34)	−0.13 (−0.38 to 0.12)	−0.25 (−0.50 to −0.00)
Adjusted for age	−0.11 (−0.38 to 0.16)	0.15 (−0.12 to 0.44)	0.04 (−0.22 to 0.30)	0.11 (−0.14 to 0.35)	−0.15 (−0.39 to 0.10)	−0.26 (−0.51 to −0.01)
Adjusted for age and sex	−0.10 (−0.38 to 0.18)	0.14 (−0.14 to 0.44)	0.03 (−0.24 to 0.30)	0.12 (−0.14 to 0.38)	−0.16 (−0.42 to 0.09)	−0.26 (−0.51 to −0.01)
Full model	−0.11 (−0.41 to 0.18)	0.15 (−0.14 to 0.47)	0.05 (−0.23 to 0.33)	0.07 (−0.19 to 0.34)	−0.11 (0.37–0.16)	−0.27 (−0.52 to −0.01)
GM CBF (ml/100g/minute)						
Crude model	0.14 (−0.11 to 0.40)	−0.17 (−0.44 to 0.08)	0.15 (−0.11 to 0.40)	−0.15 (−0.39 to 0.10)	0.17 (−0.07 to 0.42)	0.14 (−0.12 to 0.38)
Adjusted for age	0.14 (−0.13 to 0.40)	−0.16 (−0.45 to 0.10)	0.15 (−0.10 to 0.41)	−0.15 (−0.40 to 0.10)	0.18 (−0.07 to 0.42)	0.14 (−0.11 to 0.39)
Adjusted for age and sex	0.19 (−0.08 to 0.46)	−0.23 (−0.52 to 0.04)	0.13 (−0.13 to 0.39)	−0.13 (−0.38 to 0.13)	0.15 (−0.10 to 0.41)	0.14 (−0.12 to 0.38)
Full model	0.18 (−0.10 to 0.48)	−0.22 (−0.53 to 0.07)	0.14 (−0.14 to 0.42)	−0.16 (−0.42 to 0.11)	0.19 (−0.08 to 0.46)	0.14 (−0.12 to 0.40)
GM volume (%ICV)						
Crude model	−0.03 (−0.28 to 0.23)	−0.03 (−0.28 to 0.23)	−0.13 (−0.38 to 0.11)	0.04 (−0.19 to 0.25)	−0.04 (−0.25 to 0.19)	−0.16 (−0.37 to 0.09)
Adjusted for age	−0.07 (−0.33 to 0.18)	0.02 (−0.23 to 0.28)	−0.12 (−0.37 to 0.13)	0.00 (−0.21 to 0.22)	−0.00 (−0.22 to 0.22)	−0.15 (−0.36 to 0.09)
Adjusted for age and sex	−0.18 (−0.44 to 0.08)	0.14 (−0.13 to 0.41)	−0.08 (−0.33 to 0.17)	−0.07 (−0.28 to 0.16)	0.06 (−0.16 to 0.27)	−0.14 (−0.35 to 0.09)
Full model	−0.13 (−0.41 to 0.14)	0.10 (−0.18 to 0.38)	−0.06 (−0.32 to 0.19)	−0.09 (−0.31 to 0.15)	0.09 (−0.15 to 0.31)	−0.12 (−0.34 to 0.12)
Hippocampal volume (%ICV)						
Crude model	−0.03 (−0.29 to 0.22)	0.01 (−0.24 to 0.26)	−0.10 (−0.35 to 0.15)	−0.10 (−0.32 to 0.14)	0.10 (−0.14 to 0.32)	0.02 (−0.23 to 0.26)
Adjusted for age	−0.03 (−0.29 to 0.23)	0.01 (−0.26 to 0.27)	−0.10 (−0.35 to 0.15)	−0.11 (−0.33 to 0.14)	0.11 (−0.13 to 0.34)	0.02 (−0.23 to 0.27)
Adjusted for age and sex	−0.09 (−0.37 to 0.18)	0.07 (−021 to 0.36)	−0.08 (−0.33 to 0.18)	−0.15 (−0.38 to 0.10)	0.15 (−0.11 to 0.38)	0.02 (−0.23 to 0.27)
Full model	−0.08 (−0.37 to 0.20)	0.06 (−0.23 to 0.35)	−0.02 (−0.28 to 0.26)	−0.15 (−0.40 to 0.12)	0.15 (−0.11 to 0.40)	0.04 (−0.23 to 0.30)
Overall cortical thickness (mm)						
Crude model	0.17 (−0.08 to 0.42)	−0.14 (−0.40 to 0.10)	−0.08 (−0.33 to 0.17)	0.18 (−0.06 to 0.42)	−0.22 (−0.46 to 0.02)	−0.08 (−0.33 to 0.17)
Adjusted for age	0.11 (−0.14 to 0.37)	−0.09 (−0.34 to 0.17)	−0.06 (−0.31 to 0.18)	0.15 (−0.09 to 0.39)	−0.18 (−0.43 to 0.06)	−0.07 (−0.32 to 0.17)
Adjusted for age and sex	0.08 (−0.19 to 0.35)	−0.05 (−0.32 to 0.23)	−0.04 (−0.29 to 0.21)	0.13 (−0.13 to 0.38)	−0.16 (−0.42 to 0.08)	−0.07 (−0.31 to 0.18)
Full model	0.03 (−0.24 to 0.31)	−0.01 (−0.29 to 0.27)	0.01 (−0.25 to 0.27)	0.08 (−0.18 to 0.34)	−0.12 (−0.37 to 0.14)	−0.08 (−0.33 to 0.17)
WMH volume (mL)						
Crude model	−0.18 (−0.43 to 0.06)	0.17 (−0.07 to 0.42)	0.10 (−0.14 to 0.35)	0.04 (−0.20 to 0.28)	−0.05 (−0.29 to 0.19)	−0.07 (−0.32 to 0.18)
Adjusted for age	−0.08 (−0.32 to 0.15)	0.07 (−0.17 to 0.31)	0.06 (−0.17 to 0.29)	0.09 (−0.14 to 0.31)	−0.10 (−0.33 to 0.12)	−0.09 (−0.33 to 0.14)
Adjusted for age and sex	−0.11 (−0.37 to 0.14)	0.10 (−0.16 to 0.37)	0.07 (−0.17 to 0.31)	0.09 (−0.15 to 0.32)	−0.11 (−0.34 to 0.13)	−0.09 (−0.33 to 0.14)
Full model	−0.13 (−0.40 to 0.14)	0.12 (−0.15 to 0.39)	0.11 (−0.13 to 0.36)	0.10 (−0.15 to 0.34)	−0.11 (−0.35 to 0.13)	−0.07 (−0.32 to 0.17)
MSMD (mm^2/s)						
Crude model	0.16 (−0.09 to 0.40)	−0.11 (−0.35 to 0.14)	0.15 (−0.10 to 0.39)	0.07 (−0.18 to 0.31)	−0.04 (−0.28 to 0.21)	−0.13 (−0.37 to 0.13)

Continued

Table 3 Linear Regression Models Estimating the Relationships Between Omental and Subcutaneous WAT Parameters and Neuroimaging Parameters and Global Cognition *(continued)*

	Omental WAT			Subcutaneous WAT		
	Number of adipocytes per mm^2	Average diameter (μm)	CLS	Number of adipocytes per mm^2	Average diameter (μm)	CLS
	β (95% CI)	β (95% CI)	β (95% CI)	β (95% CI)	β (95% CI)	β (95% CI)
Adjusted for age	0.14 (−0.12 to 0.39)	−0.08 (−0.34 to 0.18)	0.16 (−0.09 to 0.40)	0.05 (−0.20 to 0.30)	−0.02 (−0.27 to 0.23)	−0.12 (−0.36 to 0.14)
Adjusted for age and sex	0.11 (−0.17 to 0.39)	−0.05 (−0.33 to 0.24)	0.19 (−0.07 to 0.43)	0.03 (−0.22 to 0.29)	−0.00 (−0.26 to 0.25)	−0.11 (−0.36 to 0.15)
Full model	0.12 (−0.18 to 0.41)	−0.04 (−0.34 to 0.26)	0.20 (−0.07 to 0.47)	0.06 (−0.21 to 0.33)	−0.04 (−0.30 to 0.23)	−0.13 (−0.40 to 0.14)
Compound *z* score cognition						
Crude model	−0.04 (−0.29 to 0.21)	0.03 (−0.24 to 0.29)	−0.01 (−0.27 to 0.24)	0.13 (−0.12 to 0.36)	−0.11 (−0.35 to 0.14)	0.05 (−0.20 to 0.29)
Adjusted for age	−0.07 (−0.33 to 0.19)	0.06 (−0.21 to 0.34)	0.01 (−0.25 to 0.26)	0.11 (−0.14 to 0.35)	−0.09 (−0.34 to 0.16)	0.05 (−0.19 to 0.29)
Adjusted for age and sex	−0.15 (−0.42 to 0.13)	0.14 (−0.14 to 0.43)	0.04 (−0.22 to 0.30)	0.07 (−0.18 to 0.32)	−0.06 (−0.31 to 0.19)	0.07 (−0.18 to 0.31)
Full model	−0.19 (−0.46 to 0.09)	0.16 (−0.13 to 0.44)	0.10 (−0.15 to 0.35)	0.02 (−0.22 to 0.26)	−0.03 (−0.26 to 0.21)	0.02 (−0.21 to 0.25)

Beta coefficients with 95% confidence intervals. In the full model, we adjusted for age, sex, education, HT, DM, and smoking.
Abbreviations: CBF = cerebral blood flow; CLS = crown-like structures; GM = gray matter; ICV = intracranial volume; MSMD = mean skeletonized mean diffusivity; sCoV = spatial coefficient of variation; WAT = white adipose tissue; WMH = white matter hyperintensity.

parameters and brain atrophy, WM health, and cognitive function cannot be objectified within a morbidly obese patient group alone, but only when compared with a healthy control group or increasing the range of BMI. One of the possible explanations might be a certain threshold between obesity indices and brain health. Once this threshold in BMI or WC is reached, differences in brain structure and perfusion might not be detectable anymore. One more reason might be the relatively young age of our participants to detect differences in brain imaging outcomes. Another explanation may lie in the complex link between obesity and the brain, which is far more multifaceted than the role of WAT and adipokines alone.[11] In our study, we found only a positive relationship between FPG and the sCoV in the NAcc, but no other significant associations between WAT-associated brain parameters and circulating plasma markers were observed. This suggests an important role for metabolic dysfunction in the link between obesity and brain health; however, further studies are needed to explore the interaction between WAT, glucose metabolism, and brain health. For further research, it is advised to include adipokine secretion from cultured adipocyte biopsies instead of only circulating plasma levels and to include more parameters involving the link between obesity and the brain. Such ex vivo experiments would provide information on adipokine/chemokine release per minute from WAT, which may be a more relevant metric than plasma concentrations. Another parameter to be considered is, e.g., gut microbiota, which may affect metabolism, appetite regulation, adiposity, and directly and indirectly the brain.[11]

The associations between WAT parameters and the brain were seen only for oWAT. This is in line with the literature describing that vWAT including oWAT, compared with scWAT, is strongly associated with not only systemic inflammation and obesity-associated metabolic diseases but also structural brain differences.[8,15] Within our study, the average diameter in oWAT was positively associated with sCoV in the parietal cortex and the number of adipocytes was positively associated with sCoV in the NAcc. sCoV is a sensitive parameter related to the arterial transit time (ATT), which provides information on subtle changes in cerebral hemodynamic status. A higher sCoV value is associated with a longer and irregular ATT and cerebrovascular pathology.[3,37] WAT parameters did not relate significantly with GM volume, cortical thickness, WM integrity, or cognition. Possibly, these participants were at a turning point at which only subtle cerebrovascular changes occur, but no major structural effects nor cognitive impairment yet. We found a very low WMH burden, and there were no indications for cognitive impairment based on the MoCA score. Overall, this early stage of obesity-related effects on the brain might provide an ideal time window for disease-modifying therapies to prevent further changes in brain structure and function.

In previous research, NAcc and parietal cortex were both associated with adiposity in obesity.[7,47] Especially the NAcc, which is part of the mesolimbic system and highly involved in reward and goal-directed behavior, is examined in relation to adiposity.[7] In our research, the relationship between oWAT morphology and sCoV was highly influenced by age and sex in both regions, probably because the distribution of fat differs across age and sex.[48] Men, for example, typically show more vWAT, whereas women typically accumulate more fat around the hips.[48] Earlier research also indicated a positive association between sCoV in

Figure 2 Illustrative Figure Depicting CBF (A) and Spatial Cov (B) Maps in Axial Orientation for 3 Slices

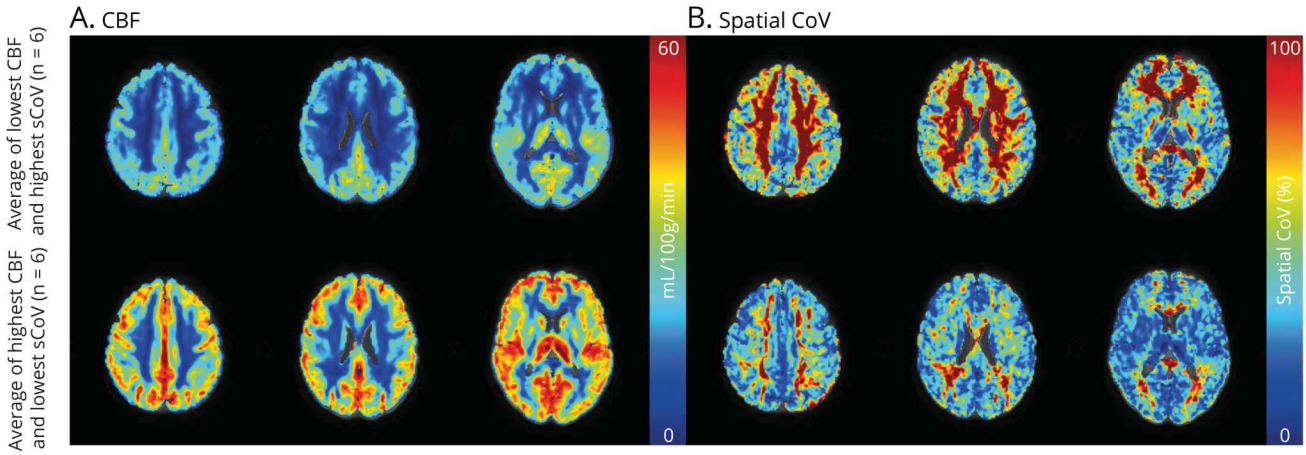

Top row, average CBF, and spatial CoV maps of 6 participants with, on average, the lowest CBF in GM and the highest sCoV in GM from the total participants studied. Bottom row, average CBF and spatial sCoV maps for 6 participants with, on average, the highest CBF in GM and the lowest sCoV in GM. Abbreviations: CBF = cerebral blood flow, sCoV = spatial coefficient of variation.

GM with age and an inverse association with sex.[38] In our study, the relationship between oWAT morphology and sCoV in the NAcc was highly influenced by sex because after adjustment these associations became nonsignificant. Unfortunately, the number of men in our study was too small to study the differences between men and women in more detail.

Furthermore, the average diameter in oWAT was inversely associated with sCoV in the NAcc and positively with sCoV in the parietal cortex. This seems contradictory; however, both hyperplasia and hypertrophy are considered detrimental, and mainly, the balance between hyperplasia and hypertrophy in oWAT and scWAT is associated with physiologic dysfunction.[12]

Table 4 Linear Regression Models Estimating the Relation Between Omental and Subcutaneous WAT Parameters and Statistically Significant ($p < 0.01$) ROIs: sCoV in the Parietal Cortex and sCoV in the Nucleus Accumbens

	Omental WAT			Subcutaneous WAT		
	Number of adipocytes per mm^2	Average diameter (μm)	CLS	Number of adipocytes per mm^2	Average diameter (μm)	CLS
	β (95% CI)	β (95% CI)	β (95% CI)	β (95% CI)	β (95% CI)	β (95% CI)
Parietal cortex sCoV (%)						
Crude model	−0.28 (−0.53 to −0.03)	0.33[a] (0.10–0.60)	0.23 (−0.02 to 0.47)	−0.15 (−0.39 to 0.10)	0.11 (−0.14 to 0.36)	−0.14 (−0.40 to 0.11)
Adjusted for age	−0.23 (−0.49 to 0.02)	0.29 (0.05–0.57)	0.20 (−0.05 to 0.44)	−0.12 (−0.36 to 0.13)	0.07 (−0.17 to 0.32)	−0.15 (−0.40 to 0.10)
Adjusted for age and sex	−0.17 (−0.43 to 0.08)	0.23 (−0.03 to 0.50)	0.15 (−0.09 to 0.39)	−0.06 (−0.30 to 0.18)	0.02 (−0.22 to 0.26)	−0.16 (−0.40 to 0.08)
Full model	−0.16 (−0.43 to 0.10)	0.22 (−0.04 to 0.51)	0.17 (−0.08 to 0.42)	−0.08 (−0.32 to 0.17)	0.05 (−0.19 to 0.30)	−0.17 (−0.42 to 0.07)
NAcc sCoV (%)						
Crude model	0.31 (0.06–0.57)	−0.27 (−0.55 to −0.02)	0.04 (−0.22 to 0.30)	−0.08 (−0.32 to 0.17)	0.11 (−0.14 to 0.35)	−0.18 (−0.46 to 0.08)
Adjusted for age	0.34[a] (0.09–0.61)	−0.30 (−0.59 to −0.05)	0.04 (−0.23 to 0.30)	−0.07 (−0.32 to 0.18)	0.11 (−0.15 to 0.35)	−0.19 (−0.47 to 0.08)
Adjusted for age and sex	0.31 (0.05–0.59)	−0.27 (−0.57 to −0.00)	0.07 (−0.20 to 0.34)	−0.11 (−0.36 to 0.15)	0.14 (−0.12 to 0.39)	−0.17 (−0.45 to 0.10)
Full model	0.34 ($p = 0.010$) (0.09–0.62)	−0.29 (−0.59 to −0.03)	0.11 (−0.16 to 0.38)	−0.06 (−0.31 to 0.19)	0.09 (−0.16 to 0.35)	−0.10 (−0.38 to 0.18)

Abbreviations: CLS = crown-like structures, sCoV = spatial coefficient of variation, NAcc = nucleus accumbent; WAT = white adipose tissue.
Beta coefficients with 95% confidence intervals. In the full model, we adjusted for age, sex, education, HT, DM, and smoking.
[a] p value < 0.01.

Figure 3 Schematic Summary of the Explored Relationships Between WAT, Circulating Plasma Markers, and Brain Structure and Perfusion

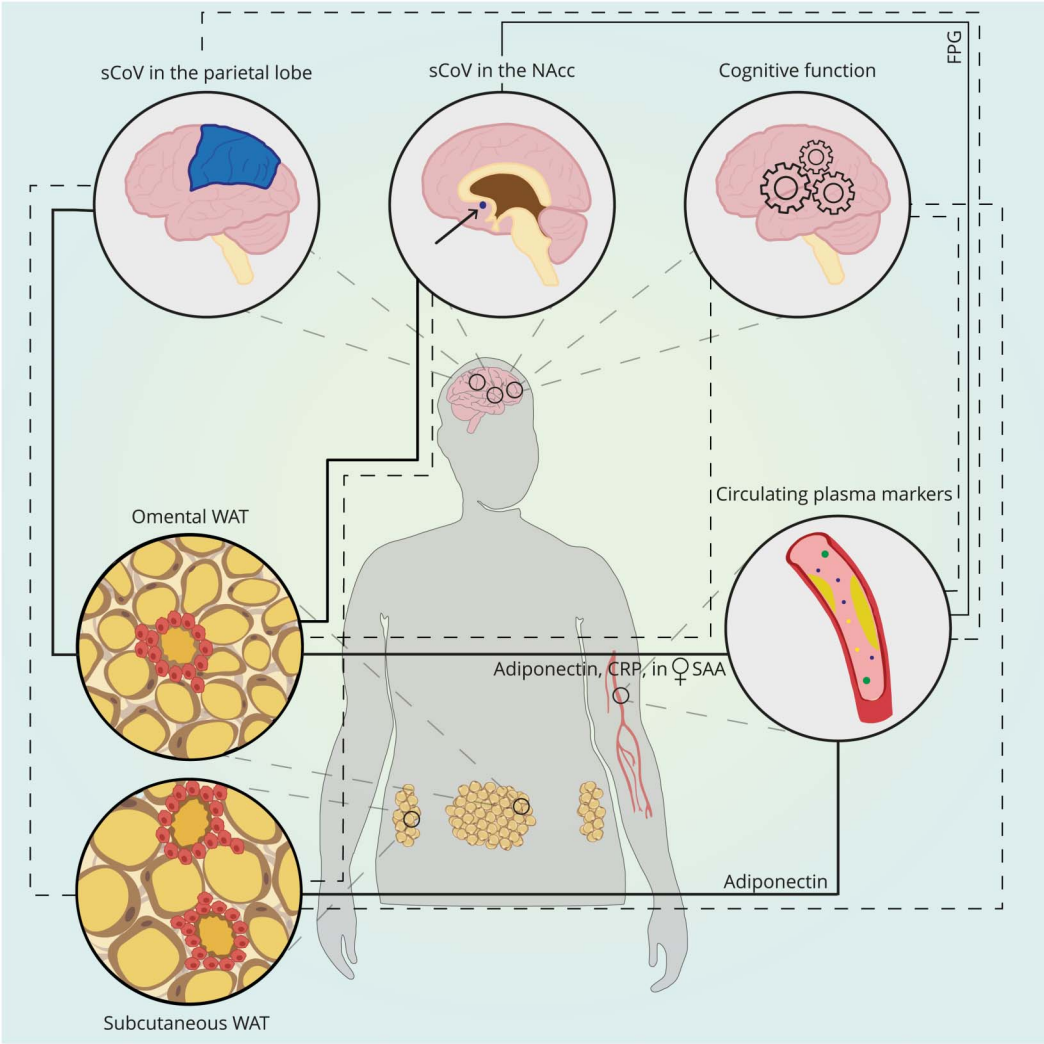

Subcutaneous WAT showed more hypertrophy and crown-like structures compared with oWAT. Subcutaneous WAT and oWAT morphology were associated with circulating adiponectin levels (inverse association between average adipocyte diameter and adiponectin). CRP was inversely associated with adipocyte number and positively with average adipocyte diameter in oWAT. In women, the average diameter of oWAT was positively associated with circulating SAA. oWAT morphology was significantly associated with sCoV in the parietal cortex and in the NAcc: the average diameter of adipocytes in oWAT was positively associated with the sCoV in the parietal cortex, and the number of adipocytes in oWAT was positively associated with sCoV in the NAcc. Subcutaneous WAT and most of the circulating plasma markers were not associated with these brain parameters (dashed lines). Only FPG was positively correlated with sCoV in the NAcc. Furthermore, both WAT depots and plasma markers were associated with cognitive function (dashed lines). For illustrative purposes, other neuroimaging outcomes, such as cerebral blood flow, brain volume, cortical thickness, and white matter hyperintensities are not included in the figure. Abbreviations: sCoV = spatial coefficients of variation; NAcc = nucleus accumbens; WAT = white adipose tissue; CRP = C-reactive protein; SAA = serum amyloid A; FPG = fasting plasma glucose; oWAT = oWAT = omental WAT.

Our study has some limitations. First, no control group was included, and we focused only on variation in individuals with severe obesity in a relatively small sample size. Hence, large differences in sCoV (see e.g., eFigure 2, links.lww.com/WNL/C471) and CBF values were observed, making it possible to study associations with WAT parameters. Our second limitation is the cross-sectional design of this study. Because it is an observational study, it is not possible to conclude causality. For both limitations it is important to note that this is an explorative study, which is part of a larger study, the BARICO study.[23] Within this study, we followed up the participants longitudinally to study the effect of weight loss after BS on brain structure and function. Furthermore, there were no *APOE* data available, and participants were relatively young to study changes in brain function and structure. However, especially in mid-life, obesity is associated with cognitive decline and the risk of developing dementia.[2] Focusing on this particular age range offers the opportunity to study the development of subtle pathologic processes that might still be reversible by weight loss. Regarding the statistical analyses, we were unfortunately unable to perform mediation analyses due to the small sample size and conducted linear regression analyses. Additional application of nonlinear modeling approaches might be considered in future research for

analyzing biological systems and biochemical kinetics due to their possible nonlinearity.[49,50] For instance, the expansion of adipocytes is nonlinearly correlated with the release of cytokines because only very large adipocytes release significant amounts of inflammatory mediators[14]; therewith, subtle interactions may be overlooked when only focusing on linear relationships. Last, we had an unequal sex distribution with more than 80% women. It is important to consider this unequal distribution when looking at the results because, for example, fat tissue distribution is different between sexes.[48] Men typically store more fat in the abdomen,[48] which also explains the higher WC observed in men compared with women in our study. In general, women show smaller adipocytes in vWAT compared with those in scWAT, whereas in men, adipocytes are more similar in size.[48] Unfortunately, the number of men in our study was too small to draw any conclusions. However, it should be emphasized that our sample is an excellent representation of the general BS population, in which 20% is male.[51]

Our analyses demonstrate differences between scWAT and oWAT depots regarding morphology, inflammation, and differences in the relationship to adipokines and cerebrovascular health. Our study shows important associations between oWAT and cerebrovascular health in obesity and provides information about underlying mechanisms between obesity and brain health. This relationship indicates an early stage of obesity-related effects on the brain. More longitudinal studies with an equal gender distribution and a larger sample size are needed to study structural and functional changes of the brain in obesity over time, including more information on underlying mechanisms such as the role of different WAT depots, metabolic dysfunction, gut microbiota, inflammation, and cerebrovascular function.

Acknowledgment

The authors thank B. Geenen and S. Martens for assistance in the quantification of CLS; W. van Duyvenvoorde and J.M. Snabel for technical support; A. Hofboer for her contribution on participant recruitment and data collection; and T.J. Aufenacker and B.P.L. Witteman for collecting the WAT depots.

Study Funding

This work is supported by a grant of the Rijnstate-Radboudumc promotion fund. The histopathologic and biochemical analyses were performed in collaboration with the Netherlands Organization for Applied Scientific Research (TNO) Metabolic Health Research (Leiden, the Netherlands) with support from TNO's Research programs Biomedical Health (PMC13), ERP Body Brain Interactions, and the Shared Research Program GLoBAL, an initiative of Radboudumc, Rijnstate, and TNO. H. Mutsaerts is supported by the Dutch Heart Foundation (03-004-2020-T049).

Disclosure

Henk-Jan M.M. Mutsaerts is supported by the Dutch Heart Foundation (03-004-2020-T049); the other authors report no disclosures relevant to the manuscript. Go to Neurology.org/N for full disclosures.

Publication History

Received by *Neurology* April 22, 2022. Accepted in final form September 23, 2022. Submitted and externally peer reviewed. The handling editor was Linda Hershey, MD, PhD, FAAN.

Appendix Authors

Name	Location	Contribution
Debby Vreeken, MSc	Department of Medical Imaging, Anatomy, Radboud university medical center, Nijmegen, The Netherlands; Department of Bariatric Surgery, Vitalys, part of Rijnstate hospital, Arnhem, The Netherlands; Donders Institute for Brain, Cognition, and Behavior and Radboudumc Alzheimer Center, Radboud university medical center, Nijmegen, The Netherlands	Drafting/revision of the article for content, including medical writing for content; major role in the acquisition of data; and analysis or interpretation of data
Florine Seidel, MSc	Department of Medical Imaging, Anatomy, Radboud university medical center, Nijmegen, The Netherlands; Donders Institute for Brain, Cognition, and Behavior and Radboudumc Alzheimer Center, Radboud university medical center, Nijmegen, The Netherlands; Department of Metabolic Health Research, Netherlands Organisation for Applied Scientific Research (TNO), Leiden, The Netherlands	Drafting/revision of the article for content, including medical writing for content; major role in the acquisition of data
Guido de La Roij, MSc	Department of Medical Imaging, Anatomy, Radboud university medical center, Nijmegen, The Netherlands	Major role in the acquisition of data
Wouter Vening, MD	Department of Bariatric Surgery, Vitalys, part of Rijnstate hospital, Arnhem, The Netherlands	Major role in the acquisition of data
Willem A. den Hengst, MD, PhD	Department of Bariatric Surgery, Vitalys, part of Rijnstate hospital, Arnhem, The Netherlands	Major role in the acquisition of data
Lars Verschuren, PhD	Department of Microbiology and Systems Biology, Netherlands Organisation for Applied Scientific Research (TNO), Zeist, The Netherlands	Drafting/revision of the article for content, including medical writing for content; analysis or interpretation of data
Şerdar Özsezen, Msc	Department of Microbiology and Systems Biology, Netherlands Organisation for Applied Scientific Research (TNO), Zeist, The Netherlands	Drafting/revision of the article for content, including medical writing for content; analysis or interpretation of data
Roy P.C. Kessels, PhD	Donders Institute for Brain, Cognition, and Behavior and Radboudumc Alzheimer Center, Radboud university medical center, Nijmegen, The Netherlands; Vincent van Gogh Institute for Psychiatry, Venray, The Netherlands; Department of Medical Psychology and Radboudumc Alzheimer Center, Radboud university medical center, Nijmegen, The Netherlands	Drafting/revision of the article for content, including medical writing for content

Appendix *(continued)*

Name	Location	Contribution
Marco Duering, Prof	Medical Image Analysis Center (MIAC) and qbig, and Department of Biomedical Engineering, University of Basel, Basel, Switzerland	Drafting/revision of the article for content, including medical writing for content
Henk J.M.M. Mutsaerts, MD, PhD	Department of Radiology and Nuclear Medicine, Amsterdam UMC, Amsterdam Neuroscience, Amsterdam, The Netherlands	Drafting/revision of the article for content, including medical writing for content
Robert Kleemann, PhD	Department of Metabolic Health Research, Netherlands Organisation for Applied Scientific Research (TNO), Leiden, The Netherlands	Drafting/revision of the article for content, including medical writing for content
Maximilian Wiesmann, PhD	Department of Medical Imaging, Anatomy, Radboud university medical center, Nijmegen, The Netherlands; Donders Institute for Brain, Cognition, and Behavior and Radboudumc Alzheimer Center, Radboud university medical center, Nijmegen, The Netherlands	Drafting/revision of the article for content, including medical writing for content; Analysis or interpretation of data
Eric J. Hazebroek, MD, PhD	Department of Bariatric Surgery, Vitalys, part of Rijnstate hospital, Arnhem, The Netherlands; Division of Human Nutrition and Health, Wageningen University, Wageningen, The Netherlands	Drafting/revision of the article for content, including medical writing for content; study concept or design
Amanda J. Kiliaan, PhD	Department of Medical Imaging, Anatomy, Radboud university medical center, Nijmegen, The Netherlands; Donders Institute for Brain, Cognition, and Behavior and Radboudumc Alzheimer Center, Radboud university medical center, Nijmegen, The Netherlands	Drafting/revision of the article for content, including medical writing for content; study concept or design; and analysis or interpretation of data

References

1. WHO. *Obesity and overweight; Fact Sheet [online]*. Available at: who.int/news-room/fact-sheets/detail/obesity-and-overweight. Accessed December 2021.
2. Kiliaan AJ, Arnoldussen IAC, Gustafson DR. Adipokines: a link between obesity and dementia? *Lancet Neurol.* 2014;13(9):913-923. doi: 10.1016/s1474-4422(14)70085-7
3. Morgan CA, Melzer TR, Roberts RP, et al. Spatial variation of perfusion MRI reflects cognitive decline in mild cognitive impairment and early dementia. *Sci Rep.* 2021;11(1):23325. doi: 10.1038/s41598-021-02313-z
4. Dorrance AM, Matin N, Pires PW. The effects of obesity on the cerebral vasculature. *Curr Vasc Pharmacol.* 2014;12(3):462-472. doi: 10.2174/15701611126661404232224l1
5. Hamer M, Batty GD. Association of body mass index and waist-to-hip ratio with brain structure: UK Biobank study. *Neurology.* 2019;92(6):e594-e600. doi: 10.1212/wnl.0000000000006879
6. Shaw ME, Sachdev PS, Abhayaratna W, Anstey KJ, Cherbuin N. Body mass index is associated with cortical thinning with different patterns in mid- and late-life. *Int J Obes (Lond).* 2018;42(3):455-461. doi: 10.1038/ijo.2017.254
7. Garcia-Garcia I, Morys F, Dagher A. Nucleus accumbens volume is related to obesity measures in an age-dependent fashion. *J Neuroendocrinol.* 2020;32(12):e12812. doi: 10.1111/jne.12812.
8. Debette S, Beiser A, Hoffmann U, et al. Visceral fat is associated with lower brain volume in healthy middle-aged adults. *Ann Neurol.* 2010;68(2):136-144. doi: 10.1002/ana.22062.
9. Lampe L, Zhang R, Beyer F, et al. Visceral obesity relates to deep white matter hyperintensities via inflammation. *Ann Neurol.* 2019;85(2):194-203. doi: 10.1002/ana.25396.
10. Stanek KM, Grieve SM, Brickman AM, et al. Obesity is associated with reduced white matter integrity in otherwise healthy adults. *Obesity.* 2011;19(3):500-504. doi: 10.1038/oby.2010.312.
11. Olsthoorn L, Vreeken D, Kiliaan AJ. Gut microbiome, inflammation, and cerebrovascular function: link between obesity and cognition. *Front Neurosci.* 2021;15:761456. doi: 10.3389/fnins.2021.761456.
12. Cypess AM. Reassessing human adipose tissue. *N Engl J Med.* 2022;386(8):768-779. doi: 10.1056/nejmra2032804.
13. Kranendonk ME, van Herwaarden JA, Stupkova T, et al. Inflammatory characteristics of distinct abdominal adipose tissue depots relate differently to metabolic risk factors for cardiovascular disease: distinct fat depots and vascular risk factors. *Atherosclerosis.* 2015;239(2):419-427. doi: 10.1016/j.atherosclerosis.2015.01.035.
14. Skurk T, Alberti-Huber C, Herder C, Hauner H. Relationship between adipocyte size and adipokine expression and secretion. *J Clin Endocrinol Metab.* 2007;92(3):1023-1033. doi: 10.1210/jc.2006-1055.
15. Fontana L, Eagon JC, Trujillo ME, Scherer PE, Klein S. Visceral fat adipokine secretion is associated with systemic inflammation in obese humans. *Diabetes.* 2007;56(4):1010-1013. doi: 10.2337/db06-1656.
16. Rocha VZ, Folco EJ. Inflammatory concepts of obesity. *Int J Inflamm.* 2011;2011:529061. doi: 10.4061/2011/529061.
17. King VL, Thompson J, Tannock LR. Serum amyloid A in atherosclerosis. *Curr Opin Lipidol.* 2011;22(4):302-307. doi: 10.1097/mol.0b013e3283488c39.
18. Fang L, Guo F, Zhou L, Stahl R, Grams J. The cell size and distribution of adipocytes from subcutaneous and visceral fat is associated with type 2 diabetes mellitus in humans. *Adipocyte.* 2015;4(4):273-279. doi: 10.1080/21623945.2015.1034920.
19. Suarez-Cuenca JA, De La Pena-Sosa G, De La Vega-Moreno K, et al. Enlarged adipocytes from subcutaneous vs. visceral adipose tissue differentially contribute to metabolic dysfunction and atherogenic risk of patients with obesity. *Sci Rep.* 2021;11(1):1831. doi: 10.1038/s41598-021-81289-2.
20. Cancello R, Tordjman J, Poitou C, et al. Increased infiltration of macrophages in omental adipose tissue is associated with marked hepatic lesions in morbid human obesity. *Diabetes.* 2006;55(6):1554-1561. doi: 10.2337/db06-0133.
21. Lesna IK, Cejkova S, Kralova A, et al. Human adipose tissue accumulation is associated with pro-inflammatory changes in subcutaneous rather than visceral adipose tissue. *Nutr Diabetes.* 2017;7(4):e264. doi: 10.1038/nutd.2017.15.
22. Verboven K, Wouters K, Gaens K, et al. Abdominal subcutaneous and visceral adipocyte size, lipolysis and inflammation relate to insulin resistance in male obese humans. *Sci Rep.* 2018;8(1):4677. doi: 10.1038/s41598-018-22962-x.
23. Vreeken D, Wiesmann M, Deden LN, et al. Study rationale and protocol of the BARICO study: a longitudinal, prospective, observational study to evaluate the effects of weight loss on brain function and structure after bariatric surgery. *BMJ Open.* 2019;9(1):e025464. doi: 10.1136/bmjopen-2018-025464.
24. Galarraga M, Campion J, Munoz-Barrutia A, et al. Adiposoft: automated software for the analysis of white adipose tissue cellularity in histological sections. *J Lipid Res.* 2012;53(12):2791-2796. doi: 10.1194/jlr.d023788.
25. Freesurfer image analysis suite. surfer.nmr.mgh.harvard.edu
26. Fischl B, Dale AM. Measuring the thickness of the human cerebral cortex from magnetic resonance images. *Proc Natl Acad Sci U S A.* 2000;97(20):11050-11055. doi: 10.1073/pnas.200033797.
27. Desikan RS, Segonne F, Fischl B, et al. An automated labeling system for subdividing the human cerebral cortex on MRI scans into gyral based regions of interest. *Neuroimage.* 2006;31(3):968-980. doi: 10.1016/j.neuroimage.2006.01.021.
28. Wardlaw JM, Smith EE, Biessels GJ, et al. Neuroimaging standards for research into small vessel disease and its contribution to ageing and neurodegeneration. *Lancet Neurol.* 2013;12(8):822-838. doi: 10.1016/s1474-4422(13)70124-8.
29. Andermatt S, Pezold S, Cattin PC. Automated segmentation of multiple sclerosis lesions using multi-dimensional gated recurrent units. In: Crimi A, Bakas S, Kuijf H, Menze B, Reyes M, editors. *Brainlesion: Glioma, Multiple Sclerosis, Stroke and Traumatic Brain Injuries*: Springer International Publishing; 2018:31-42.
30. Smith SM, Jenkinson M, Woolrich MW, et al. Advances in functional and structural MR image analysis and implementation as FSL. *Neuroimage.* 2004;23(suppl 1):S208-S219. doi: 10.1016/j.neuroimage.2004.07.051.
31. Veraart J, Novikov DS, Christiaens D, Ades-Aron B, Sijbers J, Fieremans E. Denoising of diffusion MRI using random matrix theory. *Neuroimage.* 2016;142:394-406. doi: 10.1016/j.neuroimage.2016.08.016
32. Veraart J, Fieremans E, Novikov DS. Diffusion MRI noise mapping using random matrix theory. *Magn Reson Med.* 2016;76(5):1582-1593. doi: 10.1002/mrm.26059
33. Cordero-Grande L, Christiaens D, Hutter J, Price AN, Hajnal JV. Complex diffusion-weighted image estimation via matrix recovery under general noise models. *Neuroimage.* 2019;200:391-404. doi: 10.1016/j.neuroimage.2019.06.039
34. Kellner E, Dhital B, Kiselev VG, Reisert M. Gibbs-ringing artifact removal based on local subvoxel-shifts. *Magn Reson Med.* 2016;76(5):1574-1581. doi: 10.1002/mrm.26054
35. PSMD marker [online]. Available at: psmd-marker.com
36. Baykara E, Gesierich B, Adam R, et al. A novel imaging marker for small vessel disease based on skeletonization of white matter tracts and diffusion histograms. *Ann Neurol.* 2016;80(4):581-592. doi: 10.1002/ana.24758
37. Mutsaerts HJ, Petr J, Groot P, et al. ExploreASL: an image processing pipeline for multi-center ASL perfusion MRI studies. *Neuroimage.* 2020;219:117031. doi: 10.1016/j.neuroimage.2020.117031
38. Mutsaerts HJ, Petr J, Vaclavu L, et al. The spatial coefficient of variation in arterial spin labeling cerebral blood flow images. *J Cereb Blood Flow Metab.* 2017;37(9):3184-3192. doi: 10.1177/0271678x16683690
39. Mazziotta J, Toga A, Evans A, et al. A probabilistic atlas and reference system for the human brain: international Consortium for Brain Mapping (ICBM). *Philos Trans R Soc Lond Ser B: Biol Sci.* 2001;356(1412):1293-1322. doi: 10.1098/rstb.2001.0915

40. Nasreddine ZS, Phillips NA, Bédirian V, et al. The Montreal Cognitive Assessment, MoCA: a brief screening tool for mild cognitive impairment. *J Am Geriatr Soc.* 2005; 53(4):695-699. doi: 10.1111/j.1532-5415.2005.53221.x
41. Wechsler D. Wechsler *Adult Intelligence Scale-Fourth Edition (WAIS-IV)*. San Antonio, TX: NCS Pearson. 2008;22(498):1
42. Wilson BA, Cockburn J, Baddeley AD. *The Rivermead Behavioural Memory Test*. Thames Valley Test Company; 1991.
43. Schmand B, Groenink SC, van den Dungen M. [Letter fluency: psychometric properties and Dutch normative data]. *Tijdschrift voor gerontologie en geriatrie.* 2008; 39(2):64-76. doi: 10.1007/bf03078128
44. Zimmermann PG, Fimm B. Exercise care in using UAPs (unlicensed assistive personnel): a cautionary tale. *ED Management.* 1995;7(7):76-77.
45. Verhage F. *Intelligentie en leeftijd: Onderzoek bij Nederlanders van twaalf tot zevenenzeventig jaar*. Van Gorcum; 19641-98.
46. Mulder P, Morrison MC, Verschuren L, et al. Reduction of obesity-associated white adipose tissue inflammation by rosiglitazone is associated with reduced non-alcoholic fatty liver disease in LDLr-deficient mice. *Sci Rep.* 2016;6(1):31542. doi: 10.1038/srep31542
47. Karhunen LJ, Lappalainen RI, Vanninen EJ, Kuikka JT, Uusitupa MI. Regional cerebral blood flow during food exposure in obese and normal-weight women. *Brain.* 1997;120(9):1675-1684. doi: 10.1093/brain/120.9.1675
48. Lee MJ, Wu Y, Fried SK. Adipose tissue heterogeneity: implication of depot differences in adipose tissue for obesity complications. *Mol Aspects Med.* 2013;34(1):1-11. doi: 10.1016/j.mam.2012.10.001
49. Janson NB. Non-linear dynamics of biological systems. *Contemp Phys.* 2012;53(2): 137-168. doi: 10.1080/00107514.2011.644441
50. Jiang J, Lai YC. Irrelevance of linear controllability to nonlinear dynamical networks. *Nat Commun.* 2019;10(1):3961. doi: 10.1038/s41467-019-11822-5
51. Young MT, Phelan MJ, Nguyen NT. A decade analysis of trends and outcomes of male vs female patients who underwent bariatric surgery. *J Am Coll Surgeons.* 2016; 222(3):226-231. doi: 10.1016/j.jamcollsurg.2015.11.033